tributions include an $h_{O_{eff}}$ term which is the h_{OgO} contribution for oxygen participating in the surface reaction; the remaining two terms together imply the gaseous heat of reaction seen by the layer when a solid deposit is involved.

References

[1] Kaufman, L. and Nesor, H., "Stability Characterization of Refractory Materials Under High Velocity Atmospheric Flight Conditions," AFML-TR-69-84, Pt. I, Vol. I, March 1970, ManLabs Inc., Cambridge, Mass.

[2] Bernstein, H. and Baron, J. R., "Stability Characterization of Refractory Materials Under High Velocity Atmospheric Flight Conditions," AFML-TR-69-84, Pt. IV, Vol. II, Dec. 1969, ManLabs Inc., Cambridge, Mass.

[3] Scala, S. M., "The Ablation of Graphite in Dissociated Air," Paper 62-154, 1962, IAS.

[4] Gilbert, L. M., "The Hypersonic Diffusion Controlled Oxidation of Tungsten," Rept. R67SD38, 1967, General Electric Co., King of Prussia, Pa.

[5] Welsh, W. E. and Chung, P. M., "A Modified Theory for the Effect of Surface Temperature on the Combustion Rate of Carbon Surfaces in Air," *Proceedings of the Heat Transfer and Fluid Mechanics Institute*, Stanford University Press, 1963, pp. 146–159.

[6] Nachtsheim, P. R., "Multicomponent Diffusion on Chemically Reacting Laminar Boundary Layers," *Proceedings of the Heat Transfer and Fluid Mechanics Institute*, Stanford University Press, 1967, pp. 58–87.

[7] Bartlett, E. P., Kendall, R. M., and Rindal, R. A., "Unified Approximation for Mixture Transport Properties for Multicomponent Boundary Layer Applications," Rept. 66-7, Pt. IV, March 1967, Aerotherm Corp., Palo Alto, Calif.

[8] JANAF Thermochemical Data, Dow Chemical Co., Midland, Mich., 1960.

[9] Hirchfelder, J. O., Curtiss, C. F., and Bird, R. B., *Molecular Theory of Gases and Liquids*, Wiley, New York, 1966.

[10] Kendall, R. M. and Bartlett, E. P., "Nonsimilar Solution of the Multicomponent Laminar Boundary Layer by an Integral Matrix Method," Rept. 66-7, Pt. III, March 1967, Aerotherm Corp., Palo Alto, Calif.

[11] Fay, J. A. and Riddell, F. R., "Theory of Stagnation Point Heat Transfer in Dissociated Air," *Journal of the Aeronautical Sciences*, Vol. 25, No. 2, Feb. 1958, pp. 73–85.

[12] Diaconis, N. S., Gorsuch, P. D., and Sheridan, R. A., "The Ablation of Graphite in Dissociated Air, Part 2, Experiment," Paper 62-155, 1962, IAS.

[13] Metzger, J. W., Engel, M. J., and Diaconis, N. S., "Oxidation and Sublimation of Graphite in Simulated Re-Entry Environments," *AIAA Journal*, Vol. 5, No. 3, March 1967, pp. 451–460.

AUGUST 1971 AIAA JOURNAL VOL. 9, NO. 8

Behavior of a Liquid Jet near the Thermodynamic Critical Region

J. A. NEWMAN* AND T. A. BRZUSTOWSKI†
University of Waterloo, Waterloo, Ontario, Canada

As thrust levels in modern rocket engines have risen, combustion chamber pressures in excess of the fuel and oxidizer critical pressures can be expected. This study concerns itself with how these particular conditions affect the atomization and mixing processes accompanying the injection of liquid propellants into a gaseous environment. The paper describes an experimental analysis in which a liquid issues into a gas whose pressure and temperature are close to (and often exceed) the liquid critical pressure and temperature. The data include observations of the geometric, dynamic, and thermal characteristics of the spray. A theoretical analysis is performed in which the two-phase spray is treated as a turbulent submerged jet. Verified mechanisms of turbulent mixing are used where possible. The equations for the constancy of mass, momentum, and energy and a modified jet propagation equation are solved numerically to yield information about the axial velocity, concentration, and temperature difference decay rates.

Nomenclature

a = liquid to environmental gas-density ratio ρ_l/ρ_s
A = area
$b_i,\bar{b}_i$ = boundary-layer thickness, b_i/r_o
$b_M,\bar{b}_M$ = main region jet radius, b_M/r_o
C = liquid to gas mass-flow-rate ratio $\dot{m}_l/\dot{m}_g$
C_l = liquid mass fraction in liquid gas mixture $\dot{m}_l/(\dot{m}_l + \dot{m}_g)$
c_p = specific heat at constant pressure
f,g,h = velocity, concentration, and temperature distribution functions
H = heat-transfer coefficient
K = $[1 - \Delta\bar{T}_m g_M(1 - S)]$
k = thermal conductivity
$\dot{m}$ = mass flow rate
Q = liquid-to-gas heat capacity ratio
P,P_r = pressure, P/Pc
$R,\bar{R}$ = jet radius (equals r_2 in initial region, b_M in main region), R/r_o
$\mathcal{R}$ = gas constant
$r,\bar{r}$ = radial coordinate, r/r_o
r_o = injector radius
$r_1,\bar{r}_1$ = location of inner boundary in initial region, r_1/r_o
$r_2,\bar{r}_2$ = location of outer boundary in initial region, r_2/r_o
r_d = droplet radius
S = liquid to environmental temperature ratio T_{lo}/T_s
t = time
T = temperature
$\Delta\bar{T}$ = $(T_s - T)/(T_s - T_{lo})$
U = axial velocity
$\bar{U}$ = U/U_o
$x,\bar{x}$ = axial coordinate, x/r_o
α = thermal diffusivity
ρ = density
σ = surface tension
μ = viscosity

Presented as Paper 70-8 at the AIAA 8th Aerospace Sciences Meeting, New York, January 19–21, 1970; submitted February 26, 1970; revision received March 4, 1971.

* Lecturer; presently Assistant Professor, Department of Mechanical Engineering, University of Ottawa. Member AIAA.

† Chairman, Department of Mechanical Engineering. Member AIAA.

$\eta = (r_2 - r)/b_i$
$\xi = r/b_M$

Subscripts

a = average quantity
c = critical
g = gas
H = at end of initial region
i = initial region
l = liquid
m = axis of jet
M = main region
n = at end of transition region
o = at orifice
s = surrounding fluid (i.e., ambient)
T = turbulent

Introduction

THE physical processes that occur when a liquid is discharged into a gaseous environment have been the subject of theoretical and experimental research for nearly 100 years.[1] As the first process to occur in a variety of flow systems (e.g., liquid-propellant rockets, jet engines, fuel-injection systems, spray devices), studies of the injection of the liquid and its subsequent atomization into droplets have greatly contributed to the understanding of their performance (e.g., combustion instability, poor combustion efficiency, etc.).

In this study, the authors have examined the behavior of a liquid jet issuing into an environment that has not been considered to date: in particular, an environment whose properties are close to the critical properties of the injected liquid. The basic intent of this study was to supply information regarding the characteristics of a spray of fuel droplets so that subsequent ignition and combustion theories can be applied in a realistic fashion.

Extensive examinations of jet disintegration have been carried out by many investigators. Most fundamental studies have been conducted using a straight, circular-cross-section delivery tube, and information about jet behavior under various circumstances has been collected via photographic means. Among the parameters that have been observed to have an effect on jet behavior are the liquid and gas physical properties (i.e., viscosity, density, surface tension), liquid-to-gas relative velocity, and orifice size.[2-6]

A few authors have considered the specific influence of fluid vaporization on the atomization process and agree that the over-all effect is small except under special circumstances.[7,8]

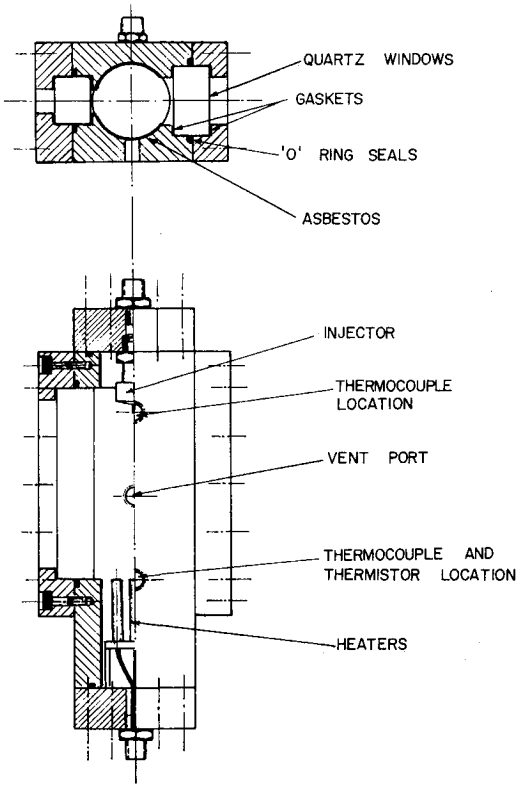

Fig. 1 Test chamber assembly.

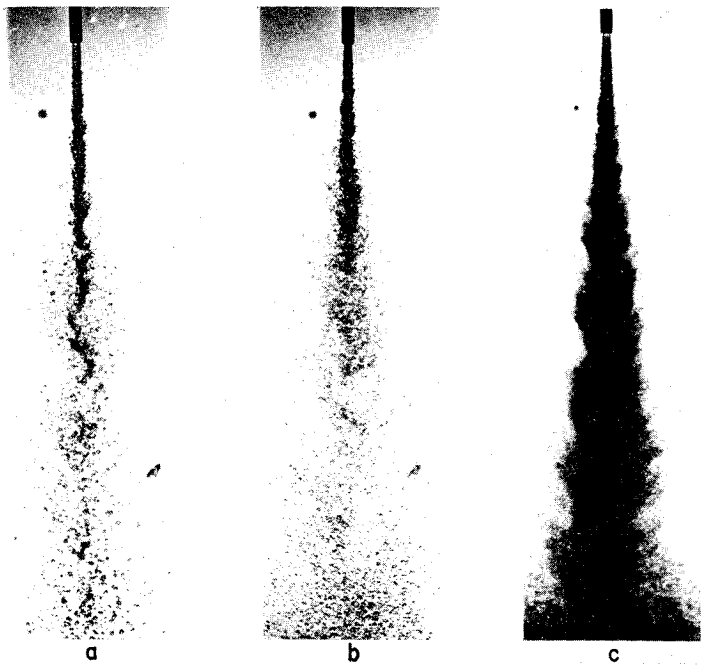

Fig. 2 Influence of gas composition on jet behavior (injection velocity = 370 cm/sec, chamber pressure = 1100 psig, environmental temperature = 22°C, partial pressure of CO_2 = a) 0 psi, b) 550 psig, c) 900 psig).

Experimental Analysis

Description of Equipment

The apparatus used in the experimental portion of this study is briefly described as follows.

A test chamber constructed of mild steel and plated with cadmium was fitted with two diametrically opposed fused quartz windows. This facilitated both visual and photographic observations of the jet. The entire chamber assembly was designed to withstand internal pressures of up to 1600 psig. Fitted near the base of the chamber were four cylindrical cartridge-type heaters. With an asbestos lining bonded to the inner wall of the chamber, temperatures in excess of 200°F were possible. The chamber temperature was monitored with chromel-alumel thermocouples and was controlled by an electronic thermostat the input to which was the signal from a thermistor located near the heaters. With this device, it was possible to control the temperature in the chamber within $\frac{1}{2}$°C. A schematic representation of the chamber assembly is given in Fig. 1.

The liquid studied in this experiment was commercial-grade carbon dioxide. CO_2 was chosen because of its availability, its low critical temperature (31°C), and because it is a fluid for which the physical properties are tabulated over a wide range of conditions. Through the use of two high-pressure regulators and a high-pressure nitrogen supply, the pressure in the test chamber and in the supply vessel could be adjusted to any desired value and maintained at that level. A valve system was incorporated into the flow system so as to control the initial CO_2/N_2 ratio in the test chamber.

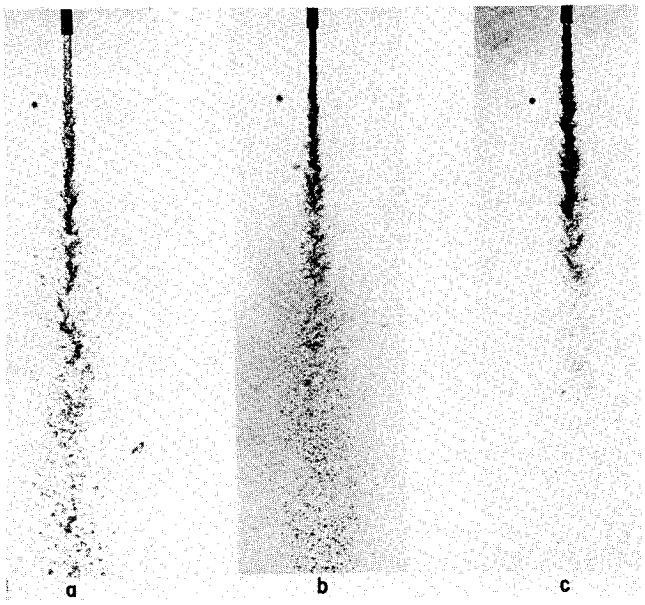

Fig. 3 Influence of gas temperature on jet behavior (injection velocity = 200 cm/sec, chamber pressure = 1300 psig, initial CO_2 partial pressure = 0 psi, environmental temperature = a) 22°C, b) 46°C, c)60°C).

The desire to do such was brought about by the need to control the evaporation rate of the "fuel."

The bulk of the experimental data was collected by photographic methods. Pictures were taken of the jet under the following sets of conditions. The chamber pressure was set to one of three values, 900 psig (reduced pressure P/P_c = 0.856), 1100 psig (P_r = 1.040), and 1300 psig (P_r = 1.228). At each of these chamber pressures, three gas compositions were considered. The ratio of the partial pressure of CO_2 to the total pressure was set to 0.0, 0.5, and to its saturation value. For each of these conditions, a number of gas temperatures were considered ranging from subcritical to supercritical. At each of the preceding settings, photographs of the jet were taken at several different velocities. Most of the observations were made with a fluid inlet temperature of 22°C and with an injector diameter of 0.66 mm.

To avoid the optically disturbing influence of refractive patterns established when droplets move through a dense gas, a blacklighting technique was used. A very short duration ($\frac{1}{2}$ μsec) light source was produced by an electronic unit. To examine the flowfield when phase change was taking place, a shadowgraph system was employed. In addition to these "action-stopping" techniques, high-speed motion pictures were taken in order to examine in detail the nature of the instability at the liquid-gas interface near the injector exit and to measure the axial velocity.

Experimental Results

At environmental pressures near the liquid critical pressure and for conditions for which no heat transfer to the liquid nor any phase change occurred, the breakup of the liquid jet was observed to be much the same as has been previously observed. At low velocities, breakup was due to capillary instability resulting in the production of large (of the same order of size as the orifice diameter) uniform droplets. This was in spite of the fact that the liquid issuing from the orifice was turbulent. Under many of the conditions encountered in this experiment, a laminar jet could not be established. The reason is simply that the minimum velocity $U_{min} = (4\sigma/\rho_l r_o)^{1/2}$ necessary to form a stable cylindrical stream[9] was greater than the velocity $U_T = 1100\ \mu_l/\rho_l r_o$ at which fluid passing through a long circular tube becomes turbulent.[10] In the case of this experimental work and in other cases for which $(\rho_l r_o \sigma/\mu_l^2)^{1/2} > 550$, the liquid jet cannot be established without it, in fact, being turbulent. As injection velocity was increased, secondary atomization began to occur until, at injection velocities above 400 cm/sec the spray became a mist of very fine droplets. (From photographic observations, droplet sizes were estimated to be of the order of 10 μ.)

The influence of gas density on the atomization process has been observed to be similar to the influence of injection velocity; i.e., the higher the gas density, the finer the spray. This effect has been reported elsewhere[5,6] for subcritical pressures and indeed appears true for supercritical pressures also.

In Figs. 2–4 are shown some example photographs that illustrate the influence of environmental gas composition and temperature on the jet's behavior. There are two main reasons why gas composition can affect the nature of the spray. The first is simply that the gas density varies with composition. The second is that the rate at which the CO_2 liquid will evaporate will depend on the amount of CO_2 vapor in the environment. All else being equal, one could expect more rapid evaporation per unit area of exposed liquid surface, the lower the CO_2 partial pressure. In Fig. 2, both the liquid and gas are at the same initial subcritical temperature of 22°C. The amount of CO_2 vapor in the gas phase, however, is different in each of the three cases shown. The pressure of 1100 psig is above the critical pressure of CO_2. The trend toward a finer, more uniform spray as CO_2 partial pressure (and hence gas density) is increased is evident. The obvious observation regarding the effect of evaporation is that the total apparent mass of liquid in the main region of the spray is less the lower the CO_2 partial pressure (i.e., the higher the evaporation rate). There are, however, several competing effects that take place under these kinds of conditions.

The time required for complete evaporation of the individual droplets within the spray will be shorter the smaller the droplets. Small droplets are produced when gas density is high, i.e., when chamber pressure is high and evaporation rates per unit area are small. It has been observed that, at pressures even higher than 1100 psig and at moderate local evaporation rates, the droplets produced can, at sufficiently high velocities, be so small that the liquid phase evaporates completely within the field of view. Unfortunately, there exists no exact analytical model that describes as a function

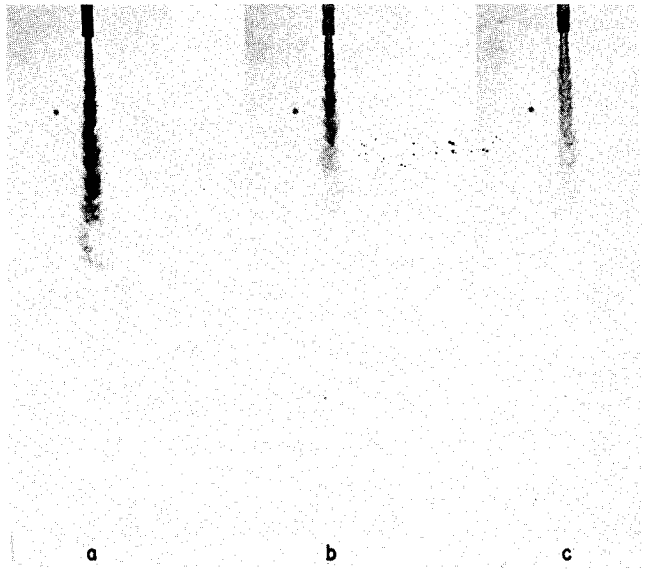

Fig. 4 Influence of chamber pressure at a supercritical temperature (injection velocity = 335 cm/sec, environmental temperature = 46°C, chamber pressure = a) 900 psig, b) 1100 psig, c) 1300 psig).

of initial droplet size the evaporation rate under these conditions. Furthermore, it is impossible to predict, as a function of injection velocity, orifice size, and gas composition, the initial droplet size distribution in the spray. Hence it is not possible at this time to make generalized statements about the total amount of liquid phase which would be present at a particular distance from the orifice.

The temperature of the gas environment will affect the jet behavior because 1) gas density decreases with increasing temperature for a fixed composition and pressure; 2) surface tension decreases with increasing temperature, becoming zero when the liquid reaches its critical temperature; and 3) evaporation rates would be expected to increase with temperature for constant liquid temperature. An example of the effect of these influences is shown in Fig. 3. Here evaporation is able to proceed rapidly in all three cases (CO_2 partial pressure is zero) and indeed would be expected to proceed at a higher rate the higher the gas temperature.

It is evident from Fig. 3 that, as temperature increases, the size and number of droplets within the spray is substantially reduced. An examination of the physical appearance of the liquid-gas interface at a short distance from the orifice suggests that the major contribution to the increased atomization efficiency is a reduction of surface tension caused by liquid heating. The decrease in the amount of liquid phase in the spray is, of course, due to phase change. The possibility of gasification (i.e., whether or not some droplets reach the liquid critical temperature) cannot be commented upon here. In this environment, where both liquid heating and evaporation can occur, the question is debatable.‡

In order to consider more specifically the possibility of gasification, a series of photographs was taken of which Fig. 4 is representative. Here there is a large percentage of CO_2 in the environment (hence evaporation is severely retarded), and the gas temperature is well in excess of the liquid critical temperature. At 900 psig, the liquid is issuing into what is essentially a superheated gas. Upon reaching its saturation temperature at this pressure, the liquid would boil. The vapor thus produced would continue to heat up to the gaseous state. The liquid cannot gasify directly, since 900 psig is subcritical. At the pressure and composition of Figs. 4b and 4c, however, the liquid cannot boil, since the chamber pressure is supercritical. The liquid droplets are simply heated until they reach the critical temperature, at which point gasification occurs.

Photographs similar to those of Figs. 4b and 4c were taken under a variety of conditions in which CO_2 partial pressure and gas temperature were high and injection velocities were sufficient to produce a finely dispersed spray. Under such conditions, it was always evident that the shape of the region in which liquid was apparent was independent of injection velocity. This observation suggests that, under these circumstances, it may be possible to describe the transfer of heat, mass, and momentum from the environment to the spray in terms of a turbulent submerged jet model. This postulate is further substantiated by the appearance of the nonevaporative spray of Fig. 2c, in which the spray boundaries closely resemble the outer boundaries of a single-phase submerged jet. The validity of this hypothesis can, however, only be verified by a comparison of computed and measured spray parameters.

In the following section, a simple theoretical analysis, appropriately modified to account for the two-phase nature of the spray will be briefly described. Following this, a comparison will be made between observed and computed mean axial velocity decay rates, spray boundaries and critical isothermal lines within the spray.

‡ In a somewhat simplified analysis of a single heptane droplet evaporating in a supercritical environment, Wieber[11] has indicated that, under certain conditions, gasification may occur before all the liquid has evaporated.

Theoretical Analysis

Model, Assumptions, and Approximations

The so-called turbulent submerged jet arises when a fluid is discharged from a nozzle into a stationary medium. The rapid motion of macroscopic lumps of fluid (eddies), moving in a disorderly fashion promotes rapid mixing between the two fluids. That is, there is a transverse transfer of heat, mass, and momentum between the discharge fluid and its surroundings. The result of these processes is the formation of a region of finite thickness (i.e., boundary layer) with a continuous distribution of mean velocity, temperature, and species concentration.

In this description of the jet, it is assumed that the boundary layer is of finite thickness; in some theories of the submerged jet, it is assumed that the boundary layer has asymptotic profiles for velocity, concentration etc. The former is chosen because of its relative mathematical simplicity and because at no time has the transport of liquid droplets beyond a well-defined boundary been observed. Other assumptions and approximations utilized in this analysis are listed, along with their qualifications as follows:

1) The gas phase obeys the ideal gas law. For the case of a hydrocarbon fuel issuing into the hot gaseous products of combustion, the approximate relation $\rho_g = P/\mathcal{R}T_g$ is quite good, since the chamber pressure, although near the critical pressure of the fuel, will generally be well below the critical pressure of the combustion products. (The critical pressure of most paraffin and aromatic fuels is about 30 atm, whereas the critical pressure of a CO_2, H_2O mixture is of the order of 150 atm.) For the conditions encountered in the experimental portions of this work, the foregoing equation is estimated to be no more than 10% in error.

2) Latent heat of vaporization is small, and evaporation rates are very low. This point has been discussed at some length by Brzustowski.[12] His discussion shows that this is a reasonable assumption at high pressures. Hence, the analysis does not consider the transfer of heat to the liquid for any purpose other than to raise the liquid temperature and, as such, will not be accurate is a highly evaporative system.

3) The liquid droplets and entrained gas have the same local mean axial velocity U. This assumption is good for small droplets (i.e. 50 μ or less).

4) Thermal equilibrium exists between the liquid droplets and the gas surrounding them. That is, the gas and liquid temperatures at any position within the spray will be equal. To consider the accuracy of this assumption requires the solution of the transient heat-transfer problem associated with a droplet moving in a gas of varying mass and temperature. This we shall not attempt to find. However, a simplified analysis can be performed to estimate these heating effects. This is shown in the Appendix. Since, in fact, the case in question is one in which the gas temperature is not constant but approaches that of the droplet the discussion in the Appendix indicates that thermal equilibration should take place no more than a few millimeters from the point where the droplets are first formed.

5) The velocity and temperature fields at the orifice exit and throughout the core region are uniform and constant. This is essentially the customary potential core assumption used in jet-flow studies. The influence of initial nonuniformities at the orifice exit have been considered[16,17] and are generally found to be slight.

6) The mean static pressure throughout the spray is constant. The system under consideration here is one in which the fluid is discharged into a large quiescent medium. The largeness of the system implies no wall effects, and hence there is no significant difference between the pressure in the jet and that of ambient pressure.

7) The effects of gravity and of molecular viscosity are small: reasonable assumptions at the high Froude and Reynolds numbers of this study.

8) The profiles of velocity, concentration, and temperature difference are each similar, i.e., the flow is self-preserving. Substantiation of this assumption has been made by considering in some detail the work of Corrsin and Uberoi.[18] In Ref. 18, consideration has been given as to whether or not similarity can be expected in a circular jet when the discharge and environmental densities are different. Their reasoning, applied to the present case, suggests that, since the density of the discharge fluid is higher than that of the environment, similarity of the flow profiles can be expected.

9) Liquid density variations are of negligible influence on the over-all spray characteristics. At supercritical environmental temperatures, liquid droplets will eventually reach their critical temperature. This will be accompanied by a marked decrease in the droplets' density. This will, however, take place in those parts of the spray where the concentration of discharge fluid is small; hence, the effect on the average density of the spray at those points will be slight.

The analysis will consider first the initial region and then the main region. The solutions to each will then be matched in the transition region.

Initial Region

At any section of the initial region, the equation describing the constancy of momentum flux, subject to the normal assumptions used in problems of free turbulent flow, can be written as

$$2\pi \int_{r_1}^{r_2} \rho_a U^2 r\, dr + \rho_l U_o^2 \pi r_1^2 = \rho_l U_0^2 \pi r_0^2 \tag{1}$$

where ρ_a, the average fluid density at any point in the mixing layer, is equal to the mass flow rate of liquid and entrained gas per unit volumetric flow rate of liquid and gas. Expressed in terms of the local liquid concentration C_l, ρ_a can be written as

$$\rho_a = \rho_l/[C_l + (\rho_l/\rho_g)(1 - C_l)] \tag{2}$$

For purposes of utilizing assumption 8, it is convenient to express temperature as

$$T = T_s[1 - \Delta\bar{T}(1 - S)] \tag{3}$$

which through the use of Eq. (2) and assumption 1, leads to

$$\rho_a = \rho_l/\{C_l + a(1 - C_l)[1 - \Delta\bar{T}(1 - S)]\} \tag{4}$$

Assuming $\bar{U} = f_i(\eta)$ $C_l = g_i(\eta)$, and $\Delta\bar{T} = h_i(\eta)$ and that ρ_l is constant Eq. (1) can be reduced quite simply to

$$\bar{r}_1^2 + 2\bar{b}_i A\bar{r}_1 + 2\bar{b}_i^2(A - B) - 1 = 0 \tag{5}$$

where

$$A = \int_0^1 \frac{f_i^2\, d\eta}{g_i + a(1 - g_i)[1 - h_i(1 - S)]}$$

$$B = \int_0^1 \frac{f_i^2 \eta\, d\eta}{g_i + a(1 - g_i)[1 - h_i(1 - S)]}$$

both of which are constants.

Equation (5) contains two unknowns (assuming A and B can be computed), $\bar{r}_1$ and $\bar{r}_2$. The relationship that determines the rate of increase of the thickness of the boundary (i.e. $\bar{r}_2 - \bar{r}_1$) with downstream distance is generally called the jet propagation equation. Its derivation for single-phase incompressible flow is based on the Prandtl hypotheses concerning the mechanisms of the turbulent expansion of a jet. Within the framework of the assumptions generally used in turbulent jet theory this equation may be written as db_i/dx = const. The constant must be determined from experimental data. From the data of Albertson et al.[19] as reported in Ref. 17, its value is about 0.27.

When the discharge and environmental fluid are of different densities, this simple relationship does not hold. However, a useful approximation for this case, introduced by Yakovlevskiy,[20] is

$$db_i/dx = (0.27/2)[1 + (\rho_2/\rho_1)] \tag{6}$$

where ρ_2 is the density of the environmental fluid and ρ_1 the density at the axis of the jet. In the initial region of the present case, Eq. (6) is simply

$$db_i/dx = 0.135[(a + 1)/a] = \text{const} \tag{7}$$

The preceding is admittedly a rather crude approximation. However, the results of Cleeves and Boelter[21] summarized in Abramovich[17] seem to substantiate Eq. (6), especially when $\rho_1 > \rho_2$ (which is certainly the case here).

Equations (5) and (7) are sufficient to characterize completely the initial region once suitable $f_i(\eta)$, $g_i(\eta)$, and $h_i(\eta)$ have been specified. Several functional forms are available, all of which are in some way or another approximations to reality. For the velocity profile $f_i(\eta)$, a form accredited to Schlichting[22] and referred to as the $\frac{3}{2}$ law will be chosen. Expressed as

$$f_i = 1 - (1 - \eta^{3/2})^2 \tag{8}$$

this expression has been shown to be quite reasonable in the case of a variable-density single-phase jet.[17,20]

For want of an accurate equation for $g_i(\eta)$ but guided by the work of Taylor,[23] a linear distribution of liquid concentration throughout the mixing layer will be assumed, that is,

$$g_i(\eta) = \eta \tag{9}$$

Taylor's work suggests also that the temperature difference profile $h_i(\eta)$ will be equal to η. However, in cases such as the present, in which the specific heats of the discharge and environmental fluids are different, a more realistic expression is

$$h_i = \eta/\{\eta + [(1 - \eta)/Q]\} \tag{10}$$

where Q is the average value of the ratio of the discharge fluid heat capacity to the environmental heat capacity. Equation (10), whose derivation is based largely on intuition, was compared with the results of Abramovich et al.[24] Agreement was found to be most satisfactory.

Equations (5) and (7), utilizing the preceding expressions for f_i, h_i, and g_i, have been solved numerically, and the results can be summarized as follows:

1) The slope and location of the outer boundary $\bar{r}_2$ is virtually independent of a, S, and Q.

2) Neither $\bar{r}_1$ nor $\bar{r}_2$ is a straight line but is nearly so.

3) The length of the initial region $\bar{x}_H$ increases with increasing a, decreasing S, and increasing Q. (The latter effect is significant when a is large.)

Main Region

The parameters of interest in this region of the spray are the jet radius, the axial velocity, liquid concentration, and temperature. The equations that can be utilized here are

$$db_M/dx = 0.11[1 + (\rho_g/\rho_{am})] \tag{11}$$

$$\int_0^A \rho_a U^2\, dA = \rho_l U_0^2 A_0 \tag{12}$$

$$\int_0^A \rho_{la} U\, dA = \rho_l U_0 A_0 \tag{13}$$

$$\int_0^A \rho_a U c_{pa} \Delta T\, dA = \rho_l U_0 A_0 c_{Pl_0} \Delta T_0 \tag{14}$$

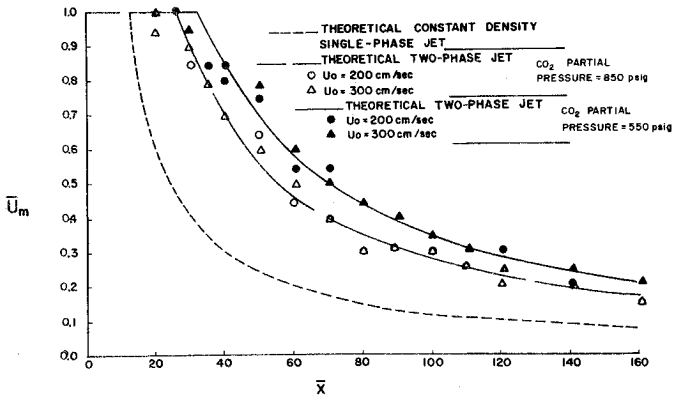

Fig. 5 Variation of mean axial velocity for isothermal spray (chamber pressure = 1100 psig).

Equation (11) is the jet propagation equation written for the main region where the empirical constant of proportionality 0.11, has been taken from the data of Förthmann.[25] ρ_{am} is the average fluid density at the jet axis. Equation (12) describes the constancy of momentum flux across any area of the main region of the spray. Equation (13) simply expresses the conservation of the mass of injected liquid, where ρ_{la} is the mass flow rate of liquid per unit volumetric flow rate of spray mixture. Equation (14) is basically the turbulent flow energy equation in which heat production by viscous action has been neglected. It is often referred to as the equation of constancy of excess heat content. The term c_{pa} is the average specific heat of the two-phase mixture and everywhere will be dependent on the specific heats of the liquid and gas and the relative amounts of each present.

Equation (11) expressed in terms of the liquid mass fraction at the jet axis C_m, the liquid-to-environmental gas-density ratio a, and invoking the ideal gas assumption, can be written as

$$\frac{db_M}{dx} = 0.11\left[1 + \frac{C_m + a[1 - \Delta\bar{T}_m(1 - S)]}{a(1 + C_m)}\right] \quad (15)$$

where

$$\Delta\bar{T}_m = (T_s - T_m)/(T_s - T_{l0})$$

According to Taylor's vorticity theorem,[23] in the main region of the jet, the velocity temperature and concentration profiles are related by $C/C_m = \Delta T/\Delta T_m = (U/U_m)^{1/2} = g_M(\xi)$, where ξ is the nondimensional radial distance from the center of the jet. Utilizing this fact and defining

$$K = [1 - \Delta\bar{T}_m g_M(1 - S)]$$

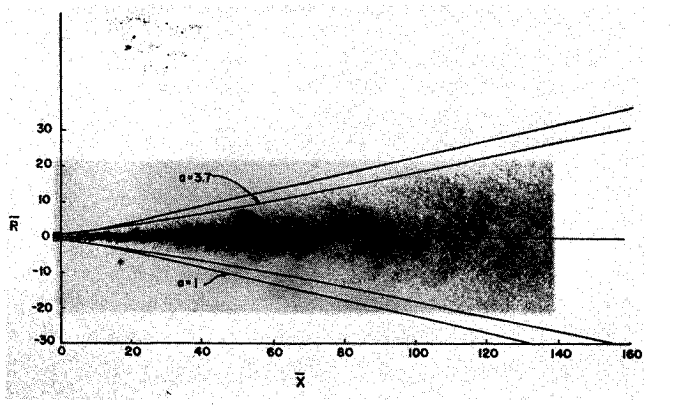

Fig. 6 Comparison between computed and observed spray boundaries for isothermal spray (injection velocity = 220 cm/sec, chamber pressure = 1100 psig, partial pressure CO_2 = 850 psig).

Eqs. (12) and (13) can be written as

$$\bar{U}_m{}^2\bar{b}_M{}^2 = 2\left\{\int_0^1 \frac{[(C_m{}^{-1}) + g_M]g_M{}^4\xi\, d\xi}{[g_M + (aK/C_m)]}\right\}^{-1} \quad (16)$$

$$\bar{U}_m\bar{b}_M{}^2 = 2\left\{\int_0^1 \frac{g_M{}^3\xi\, d\xi}{[g_M + (aK/C_m)]}\right\}^{-1} \quad (17)$$

Similarly, Eq. (14), assuming that c_{pg} is not strongly temperature-dependent, can be expressed as

$$\frac{\bar{U}_m\Delta\bar{T}_m\bar{b}_m{}^2}{Q_o} = 2\left\{\int_0^1 \frac{[Qg_M + (C_m)^{-1}]g_M{}^3\xi\, d\xi}{[g_M + (aK/C_m)]}\right\}^{-1} \quad (18)$$

where Q_o is the initial liquid-to-gas specific heat ratio. Q is the same ratio at any point in the spray and will, in general, be a function of temperature (and hence of ξ).

The four equations [(15–18)] in four unknowns ($\bar{U}_m$,$\Delta\bar{T}_m$, $\bar{b}_M$,C_m) can be solved numerically once suitable $Q(T)$ and g_M have been chosen. Again, several choices for the profile functions are available, including the somewhat cumbersome forms of Tollmein[26] and Goertler[27] and others suggested by Squire and Trouncer,[28] Townsend,[29] Hinze and van der Hegge Zijnen,[30] and Schlichting.[22] All of these forms were given consideration in this analysis. Because of its reasonable approximation to any of the foregoing and because of its relative simplicity, it was decided to again use the Schlichting $\frac{3}{2}$ law. In the main region, this is simply

$$g_M = 1 - \xi^{3/2} \quad (19)$$

It is not possible to determine experimentally the velocity and concentration profiles in this two-phase flowfield, but it is possible to measure the liquid distribution rate. At some arbitrary position in the main region of the isothermal spray, the liquid flow rate per unit area is given by

$$\rho_{la}U = \rho_l[C/(a + C)]U$$

At the jet axis, the same quantity is given by

$$(\rho_{la}U)_m = \rho_l[C_m/(a + C_m)]U_m$$

The ratio of these two expressions is

$$\frac{\dot{m}_l}{\dot{m}_{lm}} = \frac{a + C_m}{a + C}\frac{C}{C_m}\frac{U}{U_m}$$

which, through the use of Eq. (19), can be expressed as

$$\frac{\dot{m}_l}{\dot{m}_{lm}} = \frac{[(a/C_m) + 1](1 - \xi^{3/2})^3}{(a/C_m) + (1 - \xi^{3/2})}$$

This function does not produce similar profiles for the liquid distribution rate, since C_m is a function of $\bar{x}$. The accuracy of this expression, and hence to some degree of the assumed velocity and concentration profiles, was examined by collecting liquid from the spray at a number of axial and radial positions. These tests, which of course were conducted only under conditions for which phase change did not occur, indicated that indeed the assumed profile function of Eq. (19) was a reasonable approximation to reality.

Utilizing Eq. (19), Eqs. (15–18) were solved numerically for several example cases. The results, however, are of little value until they are matched to the data of the initial region. This matching is performed in the transition section.

Transition Region

The concept of a transition region is necessary since it has been assumed that the main region behaves like flow from a point source. The four governing equations place no restriction on $\bar{U}_m$ or $\Delta\bar{T}_m$, and yet it is clear that neither can exceed the value of unity. Therefore, it is necessary to define a transition section $x = x_n$ as that section of the main flow

where $\bar{U}_m = 1.0$. Similar consideration could be given to $\Delta\bar{T}_m$, leading to the definition of a thermal transition section.

It has been observed that the slope of the outer boundary of the initial region is virtually constant between $\bar{r}_2 = 1$ ($\bar{x} = 0$) and $\bar{r}_2 = \bar{r}_{2H}(\bar{x} = \bar{x}_H)$; hence a simplified expression for $\bar{x}$ in terms of $\bar{r}_2$ is

$$\bar{x} = (\bar{r}_2 - 1)[\bar{x}_H/(\bar{r}_{2H} - 1)] \qquad (20)$$

where $\bar{r}_{2H}$ and $\bar{x}_H$ are determined from Eqs. (5) and (7) with $\bar{r}_1 = 0$. Substituting $\bar{b}_{Mn}$ (determined from the main region equations with $\bar{U}_m = 1$) for $\bar{r}_2$ in Eq. (20) gives the value of $\bar{x}_n$, the distance from the orifice to the transition section. The matching of the solutions for the initial and main regions is thus accomplished.

In the following section are shown some results of these computations.

Results and Discussion

In Fig. 5, a comparison is made between computed and measured values of jet centerline velocity for two example cases. Also shown is the theoretical curve for an isothermal constant-density single-phase jet. The measured values of $\bar{U}_m$ (which were determined via high-speed picture photography) are seen to agree well with the computed $\bar{U}_m$. It should be mentioned that, at initial velocities lower than those shown and for low CO_2 partial pressure, agreement was not as good as is indicated in Fig. 5.

A comparison between the computed and observed jet radius $\bar{R}$ is shown in Fig. 6. For comparative purposes the corresponding boundaries for a single-phase constant-density jet are also shown. The two-phase jet is observed to be narrower than the single-phase jet everywhere except near the initial region where the sizes are almost the same. In addition, unlike the single-phase jet, the boundaries of the two-phase jet are not straight lines. The photograph accompanying these curves shows that the theoretical predictions are quite accurate in this case. Once again, however, in a highly evaporative system or one in which initial jet velocity was low such a comparison could not be made.

In Fig. 7 is presented the computed $\Delta\bar{T}_m$ and $\bar{R}$ for an example case in which the environmental gas temperature T_s exceeds the critical temperature of CO_2. Also shown is the calculated isotherm along which the spray temperature should equal the CO_2 critical temperature. In performing the computations for this example and for other similar cases, the specific heat of CO_2 liquid was approximated by an equation of the form.

$$c_{pl} = (A/T_l^B) + C$$

where A, B, and C are functions of pressure. In the case of Fig. 7, the region of the jet in which fluid is seen to exist in the liquid phase is quite well defined by the calculated isotherm boundary. In some other cases where the original assumptions of the theoretical analysis were not strictly adhered to, such correlation was of course not observed.

The preceding examples have been presented to give an indication of the validity of treating a two-phase spray in a near-critical environment as a process in which the governing mechanisms are those of a turbulent submerged jet. In the following section are presented some definitive conclusions that result from this study.

Conclusions

The experimental portion of this work indicates that the atomization process accompanying the injection of a liquid into a gaseous environment where the pressure is near the critical pressure of the liquid is much the same as has been observed at high but subcritical pressure by previous workers. In an isothermal nonevaporative system, the fact that the

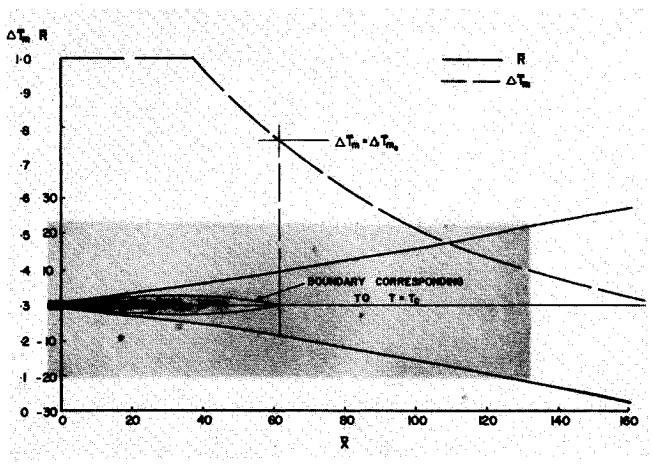

Fig. 7 Variation of axial temperature difference for supercritical environment (injection velocity = 400 cm/sec, chamber pressure = 1100 psig, partial pressure CO_2 = 550 psig, gas temperature = 60°C).

pressure may be near the thermodynamic critical pressure has no direct bearing on the atomization process. This is because atomization under these circumstances is purely a fluid-dynamic process in which a liquid interacts with a very dense gas.

The influence of environmental gas composition is reflected by the response of the spray to different local evaporation rates at different gas composition. The most significant effect is simply that at any given axial position the number density and size of the droplets are smaller the more rapid the evaporation rate. Evaporation rate decreases, of course, with increasing CO_2 in the gas phase.

At elevated temperatures and when the amount of CO_2 in the gas phase is small, liquid evaporation is somewhat enhanced. However, the dominant effect on the atomization process appears to be due to the reduction of surface tension accompanying liquid heating. This particular feature would not be so important at low pressures where surface tension is not so strongly temperature-dependent.

With a relatively high percentage of CO_2 in the gas phase and hence with relatively low local evaporation rates, supercritical environmental temperatures can result in the liquid droplets reaching their critical temperature. Under these circumstances, it is questionable whether we can refer to the flowfield as a spray. The extremely small droplets as a consequence of the very low surface tension result in a flow situation similar to that of a continuum rather than a heterogeneous liquid-gas mixture.

When local evaporation is retarded (by a high percentage of the discharge fluid in the environmental gas phase) and when jet velocity is sufficiently high to produce a uniform spray of small finely dispersed droplets, the spray can be characterized in the manner of a variable-density single-phase turbulent submerged jet. This conclusion is valid for the isothermal spray at both sub- and supercritical pressures, and, when the environmental temperature is supercritical, the model is valid for supercritical pressures. Several remarks pertinent to a fuel jet at high pressures can be made in light of this conclusion:

1) The nondimensional length of the initial region $\bar{x}_H$ increases with increasing density ratio a, decreasing S, and increasing Q.

2) The rate of decay of the nondimensional mean axial velocity $\bar{U}_m$ decreases with increasing a.

3) The jet radius $\bar{R}$ decreases with increasing a but at a slower rate as a becomes large.

4) The axial position $\bar{x}_c$ at which gasification can be expected to occur is for a given pressure and composition only slightly dependent on temperature and increases with a.

5) All the aforementioned parameters as well as $\Delta\bar{T}_m$, are independent of initial jet velocity U_o, so long as it is sufficiently high to insure that secondary atomization is the dominant form of jet breakup.

It is felt that the theoretical approach described herein can be used for design purposes if appropriate empirical relations are available for the variation of the liquid and gas physical properties. The only reservation is that in systems for which the liquid and gas specific heats are very different, the assumed temperature profile of Eq. (19) may be too narrow near the jet centerline. This would lead to a computed $\bar{x}_c$ somewhat greater than would be expected in practice.

Appendix

It is a standard result in heat transfer[13] that a sphere of radius r_d at an initial temperature T_i suddenly exposed to a fluid at constant temperature T_∞ exhibits a temperature variation of the form

$$(T_\infty - T)/(T_\infty - T_i) = f(r/r_d, Bi, Fo)$$

where Bi is the Biot number (Hr/k_l) and Fo is the Fourier number $(\alpha t/r_d)$, H being the heat-transfer coefficient, k_l the liquid thermal conductivity, α the thermal diffusivity, and t time.

For a small droplet for which heat transfer is by conduction alone, the Nusselt number $= 2Hr_d/k_g \approx 2$ and the Biot number $\approx k_g/k_l$. For the range of compositions and pressures encountered in this work, k_g/k_l is estimated to vary between $\frac{1}{2}$ and $\frac{1}{3}$.[14,15] If a liquid droplet at 22°C is exposed to gas temperatures of the order encountered in this experimental work, the time for the surface of the droplet to reach 0.99 of the gas temperature will be typically of the order $2(r_d^2/\alpha)$ hr (r_d in feet and α in square feet per hour). According to the data of Ref. 15, α should be in the neighborhood of 0.001 ft²/hr. The heatup time for droplets typically 10 μ in diameter will hence be of the order of 2 msec. To produce droplets of this size requires a jet velocity typically of the order of 400 cm/sec. Hence a droplet moving at this speed would reach 0.99 T_∞ after traveling less than 1 cm.

References

[1] Rayleigh, J. W. S., "Instability of Jets," *Proceedings of the London Mathematical Society*, Vol. 10, 1878, pp. 4–21.

[2] Haenlein, A., "Disintegration of a Liquid Jet," TM-659, 1932, NACA.

[3] Kuehn, R., "Atomization of Liquid Fuels," TM-329, 330, 331, 1925, NACA.

[4] Lee, D. W., "Photomicrographic Study of Sprays," TR-425, 1932, NACA.

[5] Muraszew, A., "Fuel Injection in Internal Combustion Engines. Spray Phenomina," Rept. 1947/R/6, 1947, Motor Industry Research Association, Great Britain.

[6] Giffin, E. and Lamb, T. A. J., "The Effect of Air Density on Spray Atomization," Rept. 1953/5, 1953, Motor Industry Research Association, Great Britain.

[7] Miesse, C. C., "Correlation of Experimental Data on the Disintegration of Liquid Jets," *Industrial and Engineering Chemistry*, Vol. 47, No. 2, Sept. 1955, pp. 1690–1701.

[8] Newman, J. A., "A Preliminary Study of the Effects of Vaporization and Transverse Oscillations on Liquid Jet Breakup," CR-72258, 1967, NASA.

[9] Schneider, J. M. and Hendricks, C. D., "Source of Uniform-Sized Liquid Drops," *Review of Scientific Instruments*, Vol. 35, 7 July 1964, pp. 1349–1350.

[10] Schiller, L. "Untersuchungen ueber Laminare und Turbulente Stroemung," *V.D.I. Forschungsarbeiten*, Vol. 248, 1922.

[11] Wieber, P. R., "Calculating Temperature Histories of Vaporizing Droplets to the Critical Point," *AIAA Journal*, Vol. 1, No. 12, Dec. 1963, pp. 2764–2769.

[12] Brzustowski, T. A., "Chemical and Physical Limits on Vapor-Phase Diffusion Flames of Droplets," *Canadian Journal of Chemical Engineering*, Vol. 43, No. 30, Feb. 1965, pp. 30–35.

[13] Rohsenow, W. M. and Choi, H., *Heat Mass and Momentum Transfer*, Prentice-Hall, New York, 1961, p. 118.

[14] *International Critical Tables*, edited by E. W. Washburn, Vol. V, McGraw-Hill, New York, p. 114.

[15] Bringer, R. P. and Smith, J. M., "Heat Transfer in the Critical Region," *AIChE Journal*, Vol. 3, No. 1, 1957, pp. 49–55.

[16] Torda, T. P., Ackerman, W. O., and Burnett, H. R., "Symmetric Turbulent Mixing of Two Parallel Streams," *Journal of Applied Mechanics*, Vol. 20, No. 1, 1953, pp. 63–71.

[17] Abramovich, G. N., *The Theory of Turbulent Jets*, translated by Scripta Technica, M.I.T. Press, Cambridge, Mass., 1963.

[18] Corrsin, S. and Uberoi, M. S., "Further Experiments on the Flow and Heat Transfer in a Heated Turbulent Air Jet," Rept. 998, 1950, NACA.

[19] Albertson, M. L., Dai, Y. B., Jensen, R. D., and Rouse, H., "Diffusion of Submerged Jets," *Proceedings of the American Society of Civil Engineers*, Vol. 74, 1948, pp. 1571–1596.

[20] Yakovlevskiy, O. V., "The Problem of the Thickness of the Turbulent Mixing Zone on the Boundary Between Two Gas Streams of Different Velocity and Density," *Izvestiya Akademii Nauk SSSR Otdelenie Tekhnicheskikh Nauk*, Vol. 10, 1958.

[21] Cleeves, V. and Boelter, L. M. K., "Isothermal and Non-Isothermal Air Jet Investigations," *Chemical Engineering Progress*, Vol. 43, No. 3, 1947, pp. 123–134.

[22] Schlichting, H., *Boundary Layer Theory*, McGraw-Hill, New York, 1960, Chap. 23, p. 590.

[23] Taylor, G. I., "The Transport of Vorticity and Heat Through Fluids in Turbulent Motion," *Proceedings of the Royal Society of London*, Vol. A 135, 1932, pp. 685–705.

[24] Abramovich, G. N., Bakulev, V. I., Golubev, V. A., and Smolin, G. G., "An Investigation into Turbulent Submerged Jets over a Wide Temperature Range," *International Journal of Heat and Mass Transfer*, Vol. 9, 1966, pp. 1047–1060.

[25] Förthmann, E., "Ueber Turbulente Strahlausbreitung," *Ingeniur Archiv*.Vol. V, 1934.

[26] Tollmein, W., "Calculation of Turbulent Expansion Process," TM 1085, NACA; translated from *Zeitschrift fuer Mathematik und Mech.*, Vol. 6, 1926.

[27] Goertler, H., "Berechnung von Aufgaben der Freien Turbulenz auf Grund Eines Neuen Naherungsansatzes," *Zeitschrift fuer Mathematik und Mech.*, Vol. 22, 1942, pp. 244–254.

[28] Squire, H. B. and Trouncer, J., "Round Jets in a General Stream," No. 1974, British Aeronautical Research Council Reports and Memos, 1944.

[29] Townsend, A. A., "The Fully Developed Turbulent Wake of a Circular Cylinder," *Australian Journal of Scientific Research*, Vol. A2, 1949, pp. 451–468.

[30] Hinze, J. O. and van der Hegge Zijnen, B. G., "Transfer of Heat and Matter in the Turbulent Mixing Zone of an Axially Symmetrical Jet," *Applied Science Research*, Vol. A1, 1949, pp. 435–461.